EPR and ENDOR Studies of Dimeric Paracyclophane Radical Cations and Dications Containing Tri- and Pentamethylene-Bridged p -Phenylene Diamine Units

7 AUTHORS, INCLUDING:

Markus Griesser
University of Ottawa
19 PUBLICATIONS **127** CITATIONS

SEE PROFILE

Stephen F Nelsen
University of Wisconsin–Madison
118 PUBLICATIONS **2,249** CITATIONS

SEE PROFILE

Georg Gescheidt
Graz University of Technology
166 PUBLICATIONS **1,660** CITATIONS

SEE PROFILE

EPR and ENDOR Studies of Dimeric Paracyclophane Radical Cations and Dications Containing Tri- and Pentamethylene-Bridged *p*-Phenylene Diamine Units

Arnulf Rosspeintner,[†] **Markus Griesser,**[†] **Isao Matsumoto,**[‡] **Yoshio Teki,**[*,‡] **Gaoquan Li,**[§] **Stephen F. Nelsen,**[*,§] **and Georg Gescheidt**[*,†]

Institute of Physical and Theoretical Chemistry, Graz University of Technology, Technikerstraße 4/I, A-8010 Graz, Department of Chemistry, Graduate School of Science, Osaka City University, 3-3-138 Sugimoto, Sumiyoshi-ku, Osaka 558 Japan, and Department of Chemistry, University of Wisconsin, Madison, Wisconsin 53706-1396

Received: January 13, 2010; Revised Manuscript Received: April 29, 2010

Solution EPR and ENDOR studies on the radical cations of three dimeric *p*-phenylene diamine (**PD**)-based compounds, the tetraisopropyl-substituted bis-trimethylene-bridged [5,5]paracyclophane **1(iPr)**[+] and its tetramethyl- and tetraisopropyl-substituted bis-pentamethylene-bridged [7,7]paracyclophane analogues **3(Me)**[+] and **3(iPr)**[+], showed that charge is localized on one **PD**[+] unit on the EPR time scale in all three compounds and determined the nitrogen splitting constants and several of the hydrogen splitting constants for these complex spectra. Rigid glass studies of the diradical dications of **1(iPr)**[2+], **3(iPr)**[2+], and its tetramethylene-bridged [6,6]paracyclophane analogue **2(iPr)**[2+], all of which show significant amounts of thermally excited triplet at low temperature, demonstrated that **1(iPr)**[2+] has a singlet ground state but the triplet lies only 0.07 kcal/mol higher in energy, and **3(iPr)**[2+] has its triplet lying 0.05 kcal/mol higher in energy than its singlet.

1. Introduction

p-Phenylene diamine (**PD**) moieties are among the most efficient (reversible) electron donating units. Such units can serve, for example, as building blocks in organic conductors such as polyaniline or redox-sensitive devices.[1−6] To assess the efficiency of such systems, the knowledge about the electron distribution in oxidized stages, particularly in the radical cations and dications, is of value. An important factor for the delocalization of the spin and the charge in such systems is their molecular topology and, presumably, the association with counterions.[3,7] It has i.a. been shown that conduction is not exclusively based on electron delocalization along conjugated π systems, but electron−hole hopping between neighboring **PD** chains, and is facilitated by dopants.[8−11]

The aspect of charge and spin delocalization between π systems that are connected by nonconjugating moieties has been addressed in investigations of various cyclophane radical cations.[12−14] It was shown that the substitution pattern and the length of the chains connecting the two electroactive moieties determine the amount of delocalization.

The **PD** derivatives introduced in this work display topologies somewhat resembling cyclophane type molecules, which can be regarded as ideal paradigms for the investigation of π stacking phenomena found, for example, in DNA.[15] When electrons are subsequently removed from such systems, radical cations and dications are formed. Although the radical cations display distinct doublet states, the electronic configurations of the dications can exist in a diamagnetic singlet, or a paramagnetic doublet (two separated radical cations) and thermally occupied triplet states.

To get insight into the interactions between the two **PD** rings in the one- and two-electron oxidized stages, this paper reports solution EPR and ENDOR studies of three radical cations obtained from dimeric **PD**-based compounds, the bis-trimethylene-bridged tetraisopropyl-substituted [5,5]paracyclophane **1(iPr)**, and the tetramethyl-substituted and tetraisopropyl-substituted bis-pentamethylene-bridged [7,7]paracyclophanes **3(Me)** and **3(iPr)**, respectively. The dications have been characterized by low-temperature EPR studies in a butyronitrile rigid-glass matrix displaying thermally occupied triplet states of the diradical dications **1(iPr)**[2+] and **3(iPr)**[2+], and their tetramethylene-bridged analogue, **2(iPr)**[2+]. We previously showed that neutral **1(Me)** and **1(Et)** exist in conformations that have the four NCCC twist angles in anti conformations, as indicated in the formulas and place the **PD** rings as far apart as possible.

1(Me) R = Me
1(Et) R = Et
1(iPr) R = iPr

2(iPr) R = iPr

3(Me) R = Me
3(iPr) R = iPr
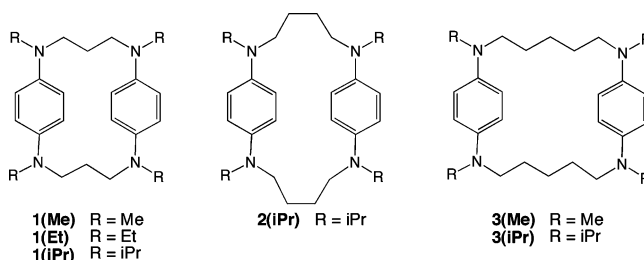
On the other hand, in the diradical dications a gauche arrangement forces the **PD**[•+] rings to lie close to each other.[16] According to the X-ray structures, the distance is significantly closer than the van der Waals contact distance in the all gauche dications, with the **PD**[•+] rings causing a strong interaction between them. Cyclic voltammetry showed that the second electron is approximately as easy to remove as the first from **1(Me)** and **1(Et)**, which points to the large and stepwise change in geometry upon double electron removal. However, the second

* To whom correspondence should be addressed. E-mail: teki@sci.osaka-cu.ac.jp (Y.T.), nelsen@chem.wisc.edu (S.F.N.), g.gescheidt-demner@tugraz.at (G.G.).
† Graz University of Technology.
‡ Osaka City University.
§ University of Wisconsin.

electron of **1(iPr)** is significantly harder to remove than the first one (0.29 V), as would be expected for a compound that did not undergo such a geometry change. Its neutral form crystallizes in a gauche,anti; gauche,anti conformation, whereas the dication crystals were in an all anti conformation.[17] Its branched alkyl groups therefore force both the neutral and dicationic forms of **1(iPr)** into other conformations than their methyl- and ethyl-substituted analogues.

This work provides experimental information related to conformations of the radical cations and establishes the amount of singlet–triplet gaps for **1(iPr)²⁺** and **3(iPr)²⁺**, mirrored by the significant triplet content. This is in contrast to **1(Me)²⁺** and **1(Et)²⁺**, which principally exist in the singlet state.[17]

2. Experimental Section

2.1. Solution EPR and ENDOR Spectra. These spectra were studied in Graz. Two Bruker X-band spectrometers, of type EMX (100 kHz field modulation) and ESP 300 (equipped with an ENDOR unit, 12.5 kHz field modulation), both with an EUROTHERM temperature control unit, were used to record the cw-EPR and ENDOR spectra. Typical experimental conditions for the EPR spectra were 2 mW microwave power and 0.1 mT field modulation.[19] The monocation EPR-spectra were obtained on solutions of the neutral compound in 1,1,1,3,3,3-hexafluoro-2-propanol (HFP, Merck, Uvasol for spectroscopy) treated with phenyl iodine bis-trifluoroacetate, (PIFA, Fluka, 95.0%), as oxidizing agent, in stoichiometric deficiency. The reagents were dissolved separately in HFP, subjected to three successive freeze–pump–thaw cycles, and subsequently mixed under reduced pressure. The hyperfine coupling constants of **1(iPr)•⁺** were calculated using the Gaussian03[20] package at the B3LYP[21,22] level of theory with the basis set 6-31G(d).[23]

2.2. Low Temperature EPR Spectra. These sepctra were studied in Osaka. For preparation of **1(iPr)²⁺**, 12.1 mg of the neutral compound are dissolved in acetonitrile, and 24.1 mg of AgSbF₆ dissolved in acetonitrile was added dropwise in a glovebox. For **3(iPr)²⁺**, 15.3 mg of neutral compound was dissolved in acetonitrile, and a solution of 23.1 mg of AgSbF₆ dissolved in acetonitrile was added dropwise in a glovebox. This reaction flask was stoppered, ultrasonicated for 5 min, and filtrated in a glovebox. The solvent was removed under vacuum. For all low-temperature EPR measurements, butyronitrile was used as the rigid glass solvent. Butyronitrile was purified with CaH₂ and distillation. Samples were degassed by repeated freeze–pump–thaw cycles. A JEOL TE300 spectrometer was used for the cw-EPR experiments. The temperature was controlled by an Oxford EPR910 cold He gas flow system. EPR signal intensity times temperature ($I_{EPR}T$) corresponds to χT, where χ is the magnetic susceptibility. The baseline for the EPR measurements is not exactly zero. The experimental data points in Figures 7 and 8 were fit to $I_{EPR}T = C/(3 + \exp(2J/T)) + A$, to obtain J, the singlet–triplet energy gap. This equation corresponds to a dimer model in which two $S = 1/2$ spins interact by $2J$.[18] Here, A is the small contribution from monocation impurity.

For the analysis of the temperature dependence, we used the signal intensity data of the $\Delta M_S = \pm 1$ allowed transitions. The EPR signal in the center of the EPR spectra of the dications stems from a monocation impurity. For the noninteracting monocation radical, $I_{EPR}(\text{monocation})T$ becomes a constant, leading to the A term.

3. Results and Discussion

3.1. Solution EPR and ENDOR Spectra. The EPR spectra obtained upon one-electron oxidation of parent **1(iPr)**, **3(Me)**,
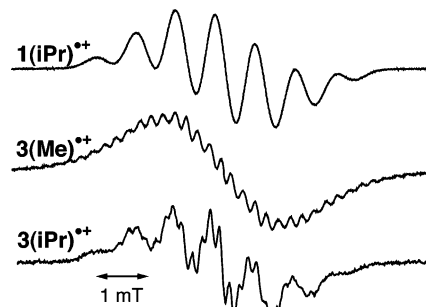

Figure 1. EPR spectra of **1(iPr)•⁺** (top), **3(Me)•⁺** (middle), and **3(iPr)•⁺** (bottom) at 293 K in HFP.

and **3(iPr)** with PIFA are compared in Figure 1. The overall widths of the spectra are almost matching. Those of the isopropyl-substituted compounds exhibit seven groups of lines corresponding to similar coupling constants for two ¹⁴N atoms (ca. 0.7 mT, Table 1) and the two β-hydrogens of the methylene groups attached to nitrogen (ca. 0.7 mT, Table 1).

The partly resolved EPR spectra can only be analyzed unambiguously with the help of ENDOR spectroscopy. In Figure 2 the EPR spectrum of **1(iPr)•⁺** is shown together with its simulation and the corresponding ENDOR spectrum. The dominating line pattern is produced by the very similar ¹⁴N hfcs of 0.74 (1 N), 0.69 (1 N) mT and ¹H hfcs of 0.79 (2 H) and 0.67 (2 H) mT. The two slightly different ¹⁴N hfcs point to the reduced symmetry being the consequence of a rather rigid arrangement of the trimethylene chains.

On the other hand, oxidation of the pentamethylene chain connected derivative **3(Me)•⁺** displays less ENDOR lines, and the dominating ¹⁴N and ¹H hfcs of 0.69 (2 N), 0.66 (6 H) and 0.38 (4 H) mT reveal higher multiplicities mirroring C_2 symmetry of this radical cation.

The simulation of the EPR signal assigned to **3(iPr)•⁺** reveals two equivalent ¹⁴N nuclei (hfc = 0.70 mT). The observation that the two β hydrogens of the methylene group adjacent to the amino nitrogen atom are distinct shows that the pentamethylene chain appears rigid on the dynamic hyperfine time scale of EPR.

To obtain more insight into the structural features of the above radical cations, the radical cations of the *N,N,N′,N′*-tetrapropyl (**TPPPD**) and the *N,N,N′,N′*-tetraisopropyl (**TiPPPD**) derivative of Wurster's Blue radical cation are chosen as paradigms.
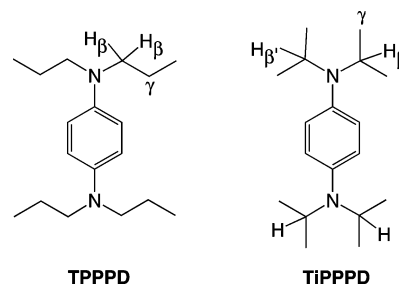

TPPPD   **TiPPPD**

For **TPPPD•⁺**, hfcs of 0.715 (2 N), 0.377 (8 H$_\beta$), 0.027 (8 H$_\gamma$), and 0.199 (4 H$_{arom.}$) mT and for **TiPPPD•⁺**, hfcs of 0.715 (2 N), 0.100 (2 H$_\beta$), 0.075 (2 H$_\beta$), 0.016 (24 H$_\gamma$), and 0.189 (4 H$_{arom.}$) mT were reported.[24] The ¹⁴N hfcs of these derivatives are essentially matching those of parent **PD•⁺** (0.700 mT). On the other hand, the hfcs attributed to the protons in the β positions are markedly smaller than those of **PD•⁺** (0.677 mT), showing that although the spin population at the nitrogen center
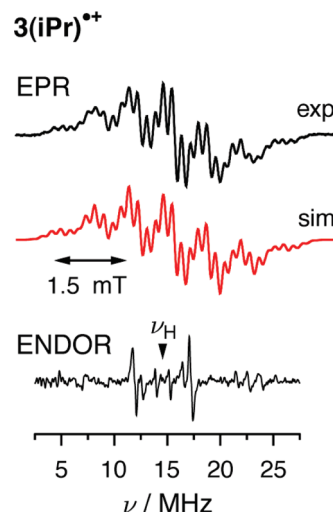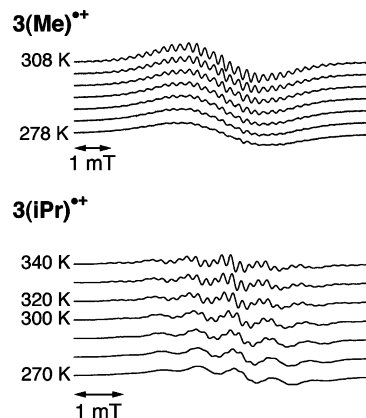
Paracyclophane Radical Cations and Dications

J. Phys. Chem. A, Vol. 114, No. 23, 2010 **6489**

TABLE 1: Hyperfine Coupling Constants (in mT) Used for the Simulation of the EPR Spectra of 1(iPr)·+, 3(Me)·+, and 3(iPr)·+ in HFP, Based on ENDOR Data and Those of Reference Compounds TPPPD and TiPPPD[a]

	1(iPr)·+	1(iPr)·+ calc.	3(Me)·+	3(iPr)·+	TPPPD·+ [c]	TiPPPD·+ [c]
g factor	2.037		2.037	2.034		
^{14}N hfc	0.74 (1)	0.69 (2)	0.69 (2)	0.70 (2)	0.715 (2)	0.715 (2)
	0.69 (1)					
^{1}H (CH$_\beta$) hfc	0.79 (1)	1.03 (2)	0.38 (4)	0.67 (2)	0.377 (8)	0.075 (2)
	0.67 (1)	0.02 (2)				0.100 (2)
^{1}H (arom.) hfc		−0.16 (2)	0.21 (4)	0.21 (4)	0.199 (4)	0.189 (4)
		−0.14 (2)				
^{1}H (CH$_3$) hfc		0.02 (12)	0.66 (6)			
^{1}H hfc[b]	0.22		0.02	0.20 (2)	0.027 (8)	0.016 (24)
	0.16			0.13 (2)		
	0.14			0.05		
	0.12			0.01		
	0.10					
	0.08					
	0.06					

[a] The ENDOR spectra were recorded at 275 K, and the EPR spectra at 295 K (340 K for **3(iPr)·+**). The numbers in parentheses are the number of equivalent nuclei used in the simulations. [b] The hfcs established by ENDOR can be tentatively assigned to more distant H nuclei of the polymethylene chains. [c] Taken from ref 24 in isopropanol/DMSO, 280 K.
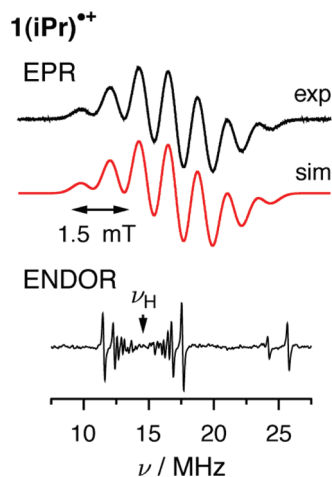
Figure 2. Experimental EPR and ENDOR spectra of **1(iPr)·+** in HFP at 295 K, compared with the EPR simulation based on the data in Table 1.
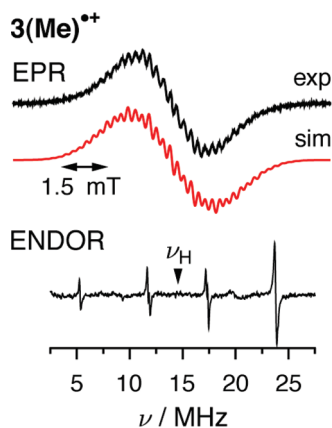
Figure 3. Experimental EPR and ENDOR spectra of **3(Me)·+** in HFP at 295 K, compared with the EPR simulation based on the data in Table 1.

Figure 4. Experimental EPR and ENDOR spectra of **3(iPr)·+** in HFP at 340 and 275 K, respectively, compared with the EPR simulation based on the data in Table 1.

Figure 5. EPR spectra of **3(Me)·+** and **3(iPr)·+** at various temperatures in HFP.

remains basically constant, the spin transfer toward the β hydrogen atoms is clearly attenuated when the methyl group is substituted with the larger propyl and the bulky isopropyl groups. This also suggests that the C_3H_8 substituents adopt rather static conformations, which, however do not disrupt the overall C_2 symmetry of these radical cations.

In the case of **1(iPr)·+**, the ^{14}N hfcs of 0.74 (1 N) and 0.69 (1 N) mT, with an average value of 0.72 mT, together with the remaining ^{1}H hfcs reveal that the electron and the charge in the cyclophane are basically confined to one **PD**-type moiety. For **3(Me)·+** and **3(iPr)·+**, compatible data can also be established (e.g., ^{14}N hfcs of 0.69 and 0.70 mT, respectively, see Table 1).

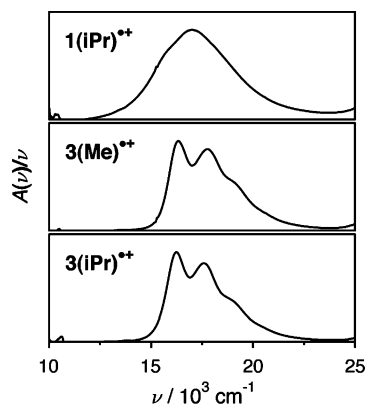**6490** *J. Phys. Chem. A, Vol. 114, No. 23, 2010*

Rosspeintner et al.

Figure 6. NIR-Vis spectra of **1(iPr)•+**, **3(Me)•+**, and **3(iPr)•+** in HFP at 293 K, obtained by oxidation of the neutral compounds with PIFA in HFP.

Accordingly, at the stage of the radical cations, electron localization onto one **PD** moiety is present for the $(CH_2)_5$ connected cyclophanes.

To test if the spin distribution is temperature dependent, EPR spectra of the flexible **3(Me)•+** and **3(iPr)•+** were taken in the temperature range between 270 and 340 K. However, apart from increasing line widths at lower temperatures (slower tumbling of the $(CH_2)_5$ chains), no alterations of the EPR spectra are notable (Figure 5).

3.2. Optical Spectra. It is important to distinguish whether the species established by EPR corresponds to that observed by optical spectroscopy. The trimethylene-bridged **1(iPr)•+** has its NIR-Vis spectrum in HFP (Figure 6) noticeably broadened compared to the N,N,N',N' tetramethyl p-phenylenediamine (**TMPD**) radical cation showing a band at 588 nm (17 000 cm^{-1}). This optical spectrum is also significantly more broadened than in acetonitrile or methylene chloride, where two maxima of similar intensity are observed.[25]

Indeed, the optical spectrum of **3(Me)•+** in HFP (Figure 6b, taken in the same cell as the EPR signal) with a maximum at 612 nm and a pronounced vibronic progression closely resembles that of the "monomeric" **TMPD•+** (band at 612 nm).[19] The NIR-Vis spectrum of **3(iPr)•+**, like its methyl-substituted analogue, strongly resembles that of **TMPD•+** (see Figure 6).

3.3. Low-Temperature EPR of Dication Diradicals in Rigid Glass. Low temperature EPR studies of **PD**-based dications on butyronitrile glass matrix revealed a significant triplet population. Dications **1(Me)2+** and **1(Et)2+** have a hardly detectable EPR signal and could not be studied at very low temperature. For **1(iPr)2•+**, the EPR signal at 100 K and its intensity dependence as a function of temperature are shown in Figure 7. The spectra were simulated with $D/hc = 0.0065$ cm^{-1} and $E/hc = 0.0$ cm^{-1}, which corresponds to a point dipole average distance between the unpaired electrons of 7.4 Å using the formula d_{pd} (Å) $= 1.3747(D/hc, cm^{-1})^{-1/3}$.[26−28] The fit of the variable temperature EPR data reveals a singlet ground state with the triplet state lying 25 cm^{-1} (0.07 kcal/mol) higher in energy (the 36 K singlet-triplet gap).

Similar data for **3(iPr)2+** are shown in Figure 8. The 0.0046 cm^{-1} value of D/hc corresponds to a point dipole average distance of 8.3 Å, and the 25 K singlet−triplet gap calculated from the temperature dependence of the EPR intensity corresponds to the triplet lying 17 cm^{-1} (0.05 kcal/mol) above the singlet.

The crystal structure of **1(iPr)2^2+**$(SbF_6^-)_2$ (which also contained solvent) shows that it exists in an all anti NCCC twist angle conformation that prevents close intramolecular contact
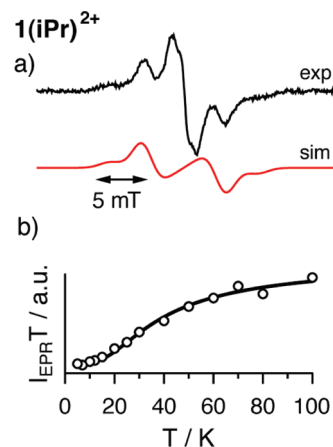

Figure 7. (a) EPR signal at 100 K and (b) dependence of the EPR signal intensity times temperature on temperature for **1(iPr)2+**$(SbF_6^-)_2$ in butyronitrile rigid-glass.
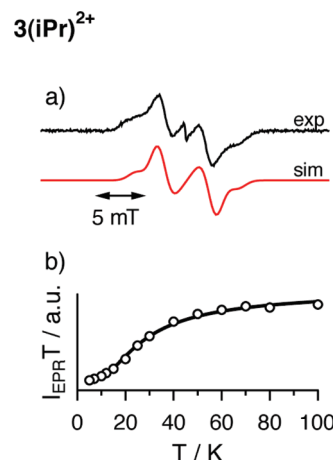

Figure 8. (a) EPR signal at 100 K and (b) dependence of the EPR signal intensity times temperature on temperature for **3(iPr)2+**$(SbF_6^-)_2$ in butyronitrile rigid-glass.

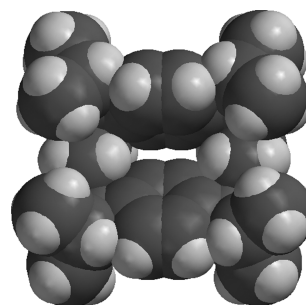**Figure 9.** View of a space-filling model of the most stable conformation calculated for the doubly $(CH_2)_4$-bridged triplet **2(iPr)2+** using molecular mechanics (Spartan02).

between the **PD** rings. Molecular mechanics calculations on the neutral precursors showed that both the $(CH_2)_4$ and $(CH_2)_5$ bridges lead to orientations with substantial distances between the **PD** moieties. Single-point B3LYP calculations carried out based on selected conformations of **3(iPr)2^2+** and the tetramethylene-bridged **2(iPr)2+** corroborated that these distances are too long to allow intramolecular van der Waals contact (see Figure 9).

EPR studies on glasses of the doubly $(CH_2)_3$, $(CH_2)_4$, and $(CH_2)_5$-bridged tetraisopropyl-substituted salts (**1(iPr)2+**, **2(iPr)2+**, and **3(iPr)2+**, respectively) near 130 K in a 1:1:1 $CH_2Cl_2/CH_3CN/CH_3(CH_2)_2CN$ glassy solvent mixture that were

Paracyclophane Radical Cations and Dications

J. Phys. Chem. A, Vol. 114, No. 23, 2010 **6491**

conducted in Madison gave spectra of triplets that are rather similar to those found in Osaka (see Figure 10). Half-field $\Delta m = 2$ absorptions were observed for these triplets.

The spectrum of $1(iPr)^{2+}$ showed significantly less resolution in the mixed solvent (Figure 10a) than in the single solvent butyronitrile rigid-glass, apparently because the monoradical impurity was considerably more intense. Failure to oxidize more completely probably occurs because of the lower redox potential of the Ag$^+$ used for carrying out the oxidation in the mixed solvent compared to CH$_2$Cl$_2$.[1] $3(iPr)^{2+}$, which is significantly easier to oxidize to the dication than is $1(iPr)^{2+}$, and showed amounts of monocation impurity that were more comparable to the results in the single solvent butyronitrile rigid-glass, and $2(iPr)^{2+}$ was only studied in the mixed solvent.

4. Conclusions

Comparing the geometries and electronic structures of the parent neutral molecules, the radical cations, and the dications, substantial rearrangements of the molecular skeletons take place during the oxidation process as mirrored by DFT calculations and X-ray structure determinations and as anticipated from cyclocvoltammetric measurements. On going from the neutral parent molecules to the radical cations, the unpaired electron resides at one **PD** moiety with the dominating portion of the spin population being located at the nitrogen atoms. Accordingly, the pyramidalization at the nitrogen atoms (of one **PD** unit) is substantially reduced. The second oxidation yields a
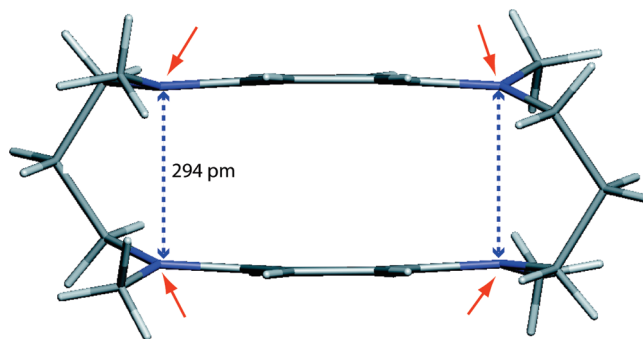

Figure 11. X-ray geometry of $1(Me)^{2+}$ (the arrows point to the nitrogen atoms).

dication comprising two essentially identical **PD$^{\bullet+}$** moieties (in an overall singlet or triplet state, see above). Here, remarkably, all four nitrogens are only slightly pyramidalized (average bond angle 119.7°, neutral: 115.9°) but in a way that the N lone pairs of the facing nitrogens are oriented toward each other. Hence, the substantial rearrangement of the cyclophanes of type **1** upon stepwise oxidation might be ascribed to a rearrangement of the trimethylene chain due to the planarization at the N centers. π Stacking phenomena may contribute to the changes in geometry as well as through-space N···N lone-pair interactions leading to (two parallel) 2c3e bonds. Analogous bonds have been established in molecules displaying similarly preoriented bis- and tetrakis(trialkylamino) moieties.[29−33]
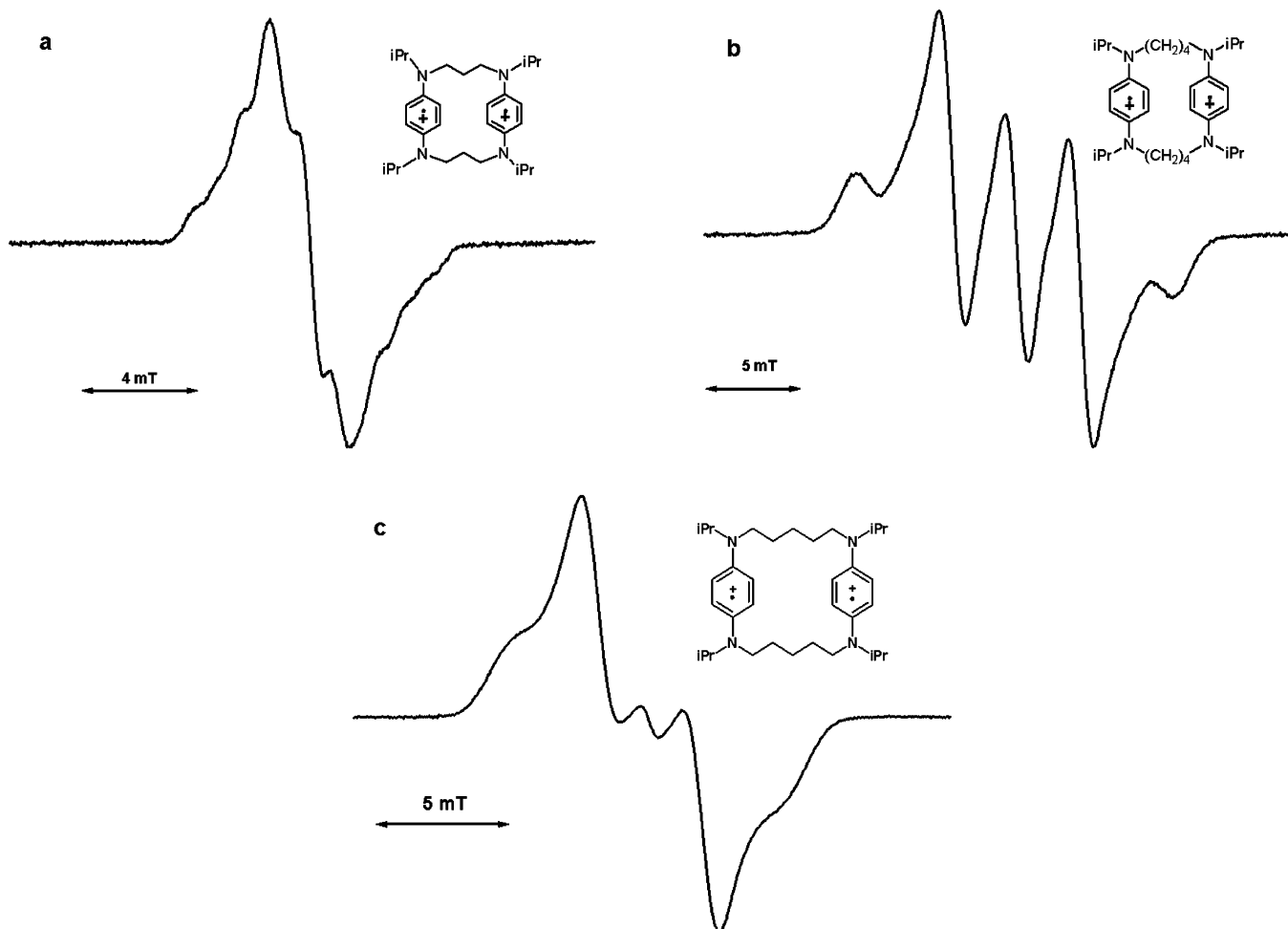

Figure 10. (a) EPR spectrum of $1(iPr)^{2+}$. (b) EPR spectrum of $2(iPr)^{2+}$. (c) EPR spectrum of $3(iPr)^{2+}$ (all spectra are taken in mixtures 1:1:1 by volume CH$_2$Cl$_2$/CH$_3$CN/CH$_3$(CH$_2$)$_2$CN).

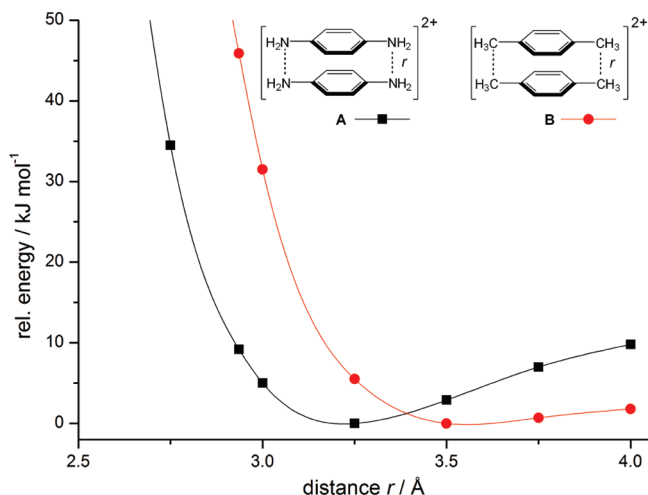**6492** *J. Phys. Chem. A, Vol. 114, No. 23, 2010*

Rosspeintner et al.

Figure 12. Distance-dependent energies for dication dimers **A** and **B** in the singlet state. The distances refer to the connections between the amino N atoms and the methyl C atoms, respectively.

To substantiate this hypotheses, we have started with the geometry (X-ray) of **1(Me)**$^{2+}$, removed the trimethylene bridges as well as the four methyl groups, and replaced them with hydrogen atoms, thus producing a **PD** dimer carrying two positive charges. The distance between the two molecules was then varied between 2.5 and 4.0 Å (without geometry optimization). Clearly, at distances of ca. 3.25 Å an energy minimum can be established (Figure 12). To distinguish between N···N and π···π interactions, we have replaced the amino by methyl groups (*p*-xylene) and performed analogous calculations. In this latter case only a minimum at a distance of ca. 3.5 Å can be found (Figure 12). This behavior holds for an overall singlet state of the **PD···PD** systems and illustrates that N···N and π···π interactions are likely to contribute to the close contact between the two **PD**$^{+•}$ moieties. In the triplet state, no minima could be found. This also explains the failure to observe distinguishable EPR spectra for **1(Me)**$^{2+}$. Moreover, these calculations suggest that the triplet-states of the dications possess geometries with larger distances between the **PD** parts. Such a geometry presumably also holds for **1(iPr)**$^{2+}$.

We also suggest from these results that close intramolecular contact of the **PD** rings in the dications with a *gg,gg* NCCC conformation is responsible for the low triplet contents that are observed for **1(Me)**$^{2+}$ and **1(Et)**$^{2+}$. Although their ground states remain singlet, **1−3(iPr)**$^{2+}$ have nearly isoenergetic singlet and triplet states because they do not achieve the close intramolecular contact, π-stacked geometry that results in strong spin-pairing.

References and Notes

(1) Sharma, G. K.; Rao, B. S. M.; O'Neill, P. *J. Phys. Chem. B* **2009**, *113*, 2207.

(2) Guo, J.; Togami, T.; Benten, H.; Ohkita, H.; Ito, S. *Chem. Phys. Lett.* **2009**, *475*, 240.

(3) Grossmann, B.; Heinze, J.; Moll, T.; Palivan, C.; Ivan, S.; Gescheidt, G. *J. Phys. Chem. B* **2004**, *108*, 4669.

(4) Zhang, J.; Barker, A. L.; Mandler, D.; Unwin, P. R. *J. Am. Chem. Soc.* **2003**, *125*, 9312.

(5) Wang, Q.; Liu, N.; Wang, X.; Li, J.; Zhao, X.; Wang, F. *Macromolecules* **2003**, *36*, 5760.

(6) Sharma, S. N.; Pillai, Z. S.; Kamat, P. V. *J. Phys. Chem. B* **2003**, *107*, 10088.

(7) Szeghalmi, A. V.; Erdmann, M.; Engel, V.; Schmitt, M.; Amthor, S.; Kriegisch, V.; Noell, G.; Stahl, R.; Lambert, C.; Leusser, D.; Stalke, D.; Zabel, M.; Popp, J. *J. Am. Chem. Soc.* **2004**, *126*, 7834.

(8) Zic, M. *J. Electroanal. Chem.* **2009**, *635*, 29.

(9) Bohli, N.; Gmati, F.; Mohamed, A. B.; Vigneras, V.; Miane, J.-L. *J. Phys. D: Appl. Phys.* **2009**, *42*, 205404/1.

(10) Klasovsky, F.; Hohmeyer, J.; Bruckner, A.; Bonifer, M.; Arras, J.; Steffan, M.; Lucas, M.; Radnik, J.; Roth, C.; Claus, P. *J. Phys. Chem. C* **2008**, *112*, 19555.

(11) Kim, J.; Park, S.; Scherer, N. F. *J. Phys. Chem. B* **2008**, *112*, 15576.

(12) Gerson, F. *Top. Curr. Chem.* **1983**, *115*, 57.

(13) Wartini, A. R.; Valenzuela, J.; Staab, H. A.; Neugebauer, F. A. *Eur. J. Org. Chem.* **1998**, 139.

(14) Huber, M.; Lendzian, F.; Lubitz, W.; Traenkle, E.; Moebius, K.; Wasielewski, M. R. *Chem. Phys. Lett.* **1986**, *132*, 467.

(15) Wagenknecht, H. A. Gray, H. *Charge Transfer in DNA: From Mechanism to Application*; Wiley-VCH: Weinheim, 2005.

(16) Nelsen, S. F.; Li, G.; Schultz, K. P.; Guzei, I. A.; Tran, H. Q.; Evans, D. A. *J. Am. Chem. Soc.* **2008**, *130*, 11620.

(17) Jalilov, A. S.; Li, G.; Nelsen, S. F.; Guzei, I.; Wu, Q. *J. Am. Chem. Soc.* **2010**, *132*, 6176.

(18) Smaller modulation amplitudes did not alter the shape of these spectra.

(19) Carlin, R. L. *Magneto-chemistry*; Springer-Verlag: Berlin, 1986.

(20) Frisch, M. J.; Trucks, G. W.; Schlegel, H. B.; Scuseria, G. E.; Robb, M. A.; Cheeseman, J. R.; Montgomery, J. A.; Jr.; Vreven, T.; Kudin, K. N.; Burant, J. C.; Millam, J. M.; Iyengar, S. S.; Tomasi, J.; Barone, V.; Mennucci, B.; Cossi, M.; Scalmani, G.; Rega, N.; Petersson, G. A.; Nakatsuji, H.; Hada, M.; Ehara, M.; Toyota, K.; Fukuda, R.; Hasegawa, J.; Ishida, M.; Nakajima, T.; Honda, Y.; Kitao, O.; Nakai, H.; Klene, M.; Li, X.; Knox, J. E.; Hratchian, H. P.; Cross, J. B.; Bakken, V.; Adamo, C.; Jaramillo, J.; Gomperts, R.; Stratmann, R. E.; Yazyev, O.; Austin, A. J.; Cammi, R.; Pomelli, C.; Ochterski, J. W.; Ayala, P. Y.; Morokuma, K.; Voth, G. A.; Salvador, P.; Dannenberg, J. J.; Zakrzewski, V. G.; Dapprich, S.; Daniels, A. D.; Strain, M. C.; Farkas, O.; Malick, D. K.; Rabuck, A. D.; Raghavachari, K.; Foresman, J. B.; Ortiz, J. V.; Cui, Q.; Baboul, A. G.; Clifford, S.; Cioslowski, J.; Stefanov, B. B.; Liu, G.; Liashenko, A.; Piskorz, P.; Komaromi, I.; Martin, R. L.; Fox, D. J.; Keith, T.; Al-Laham, M. A.; Peng, C. Y.; Nanayakkara, A.; Challacombe, M.; Gill, P. M. W.; Johnson, B.; Chen, W.; Wong, M. W.; Gonzalez, C.; Pople, J. A. *Gaussian 03, Revision E.01*; Gaussian, Inc.: Wallingford CT, 2004.

(21) Becke, A. D. *J. Chem. Phys.* **1993**, *98*, 5648.

(22) Stephens, P. J.; Devlin, F. J.; Chabalowski, C. F.; Frisch, M. J. *J. Phys. Chem.* **1994**, *98*, 11623.

(23) Hariharan, P. C.; Pople, J. A. *Theor. Chim. Acta* **1973**, *28*, 213.

(24) Grampp, G.; Kelterer, A.-M.; Landgraf, S.; Schaer, M.; Niethammer, D.; Telo, J. P.; Dias, R. M. B.; Vieira, A. J. S. C. *Monatsh. Chem.* **2005**, *136*, 519.

(25) Li, G., PhD Thesis, University of Wisconsin, 2008.

(26) Hirota, N.; Weissman, S. I. *J. Am. Chem. Soc.* **1964**, *86*, 2538.

(27) Dvolaitzky, M.; Chiarelli, R.; Rassat, A. *Angew. Chem., Int. Ed.* **1992**, *31*, 180.

(28) Connelly, N. G.; Geiger, W. E. *Chem. Rev.* **1996**, *96*, 877.

(29) Gerson, F.; Gescheidt, G.; Knoebel, J.; Martin, W. B. J.; Neumann, L.; Vogel, E. *J. Am. Chem. Soc.* **1992**, *114*, 7107.

(30) Gerson, F.; Gescheidt, G.; Buser, U.; Vogel, E.; Lex, J.; Zehnder, M.; Riesen, A. *Angew. Chem.* **1989**, *101*, 938.

(31) Exner, K.; Prinzbach, H.; Gescheidt, G.; Grossmann, B.; Heinze, J. *J. Am. Chem. Soc.* **1999**, *121*, 1964.

(32) Brouwer, A. M. *J. Phys. Chem. A* **1997**, *101*, 3626.

(33) Zwier, J. M.; Brouwer, A. M.; Keszthelyi, T.; Balakrishnan, G.; Offersgaard, J. F.; Wilbrandt, R.; Barbosa, F.; Buser, U.; Amaudrut, J.; Gescheidt, G.; Nelsen, S. F.; Little, C. D. *J. Am. Chem. Soc.* **2002**, *124*, 159.